Correlation Energy and Spin Polarization in the 2D Electron Gas

Claudio Attaccalite, Saverio Moroni, Paola Gori-Giorgi, and Giovanni B. Bachelet
INFM Center for Statistical Mechanics and Complexity and Dipartimento di Fisica, Università di Roma "La Sapienza," Piazzale A. Moro 2, 00185 Rome, Italy
(Received 26 September 2001; published 5 June 2002)

The ground-state energy of the two-dimensional uniform electron gas has been calculated with a fixed-node diffusion Monte Carlo method, including backflow correlations, for a wide range of electron densities as a function of spin polarization. We give a simple analytic representation of the correlation energy which fits our simulation data and includes several known high- and low-density limits. This parametrization provides a reliable local spin density energy functional for two-dimensional systems and an estimate for the spin susceptibility. Within the proposed model for the correlation energy, a weakly first-order polarization transition occurs shortly before Wigner crystallization as the density is lowered.

DOI: 10.1103/PhysRevLett.88.256601 PACS numbers: 72.25.–b, 02.70.Ss, 71.10.Ca, 71.15.Mb

The two-dimensional electron gas (2DEG), realized in semiconductor heterostructures [1], exhibits an extremely rich phenomenology at low density, where correlations play an important role. Being outside the reach of perturbative approaches, many crucial aspects of this interesting physics still lack a satisfactory explanation [2]. Under these circumstances, valuable information can be gained from simplified models, such as the ideal 2DEG (strictly 2D electrons interacting via a $1/r$ potential within a uniform, rigid neutralizing background). At zero temperature, the state of this system is entirely specified by the coupling parameter $r_s = 1/\sqrt{\pi n}\, a_B$, where n is the density and a_B is the Bohr radius, and the spin polarization ζ. Even for such a simple model the theory has greatly benefited from numerical work, resulting — at least for a limited range of physical properties and/or system sizes — in benchmark results, input quantities for approximate theories, and aspects of the ground-state phase diagram. The quantum Monte Carlo (QMC) method (see, e.g., Ref. [3]), for example, has accurately predicted [4,5] the critical density for Wigner crystallization of the ideal 2DEG, later observed experimentally [6], and has characterized [7] the polarization transition as being weakly first order and occurring shortly before crystallization as the density is lowered.

In this work, we present extensive QMC simulations of the liquid phase within the whole range of density and polarization, and we provide an analytic expression for the correlation energy ϵ_c as a function of r_s *and* ζ. Previous estimates of the ζ dependence were based on interpolation conjectures between the energy of the paramagnetic and of the fully polarized liquid [4,8], but, as shown later, these estimates may significantly depart from the calculated energy at intermediate polarization.

The interest in the ζ dependence stems from its use in the spin-density functional theory of two-dimensional systems [8–10], in the development of density functionals in the presence of magnetic fields [11], and, more generally, in the study of the spin-polarization transition, whose role on transport properties [2] is prompting intense experimental investigation [12].

Our combination of numerical results and known analytic properties yields an estimate of the paramagnetic susceptibility. At low density, this is an extremely difficult quantity to evaluate with approximate theories [13] due to the need of disentangling the tiny — but important — effect of quantum statistics from the huge effect of correlation. Finally, since we include the effect of backflow correlations [14] as explained below, our $\epsilon_c(r_s, \zeta)$ provides a more accurate phase diagram than previously reported [4,5]. Hartree atomic units are used throughout this work.

Numerical results.— Our calculations use standard fixed-node diffusion Monte Carlo (FN-DMC) [3], which projects the lowest-energy eigenstate Φ of the many-body Hamiltonian with the boundary condition that Φ vanishes at the nodes of a trial function Ψ. The algorithm simulates the imaginary-time evolution by a branching random walk of M copies of the N-electron system, using a short-time approximation of the importance-sampled Green's function [3]. For each of the densities corresponding to $r_s = 1, 2, 5, 10$ we have considered about 20 values of N [15] and 10–12 polarizations $\zeta = (N^{\uparrow} - N^{\downarrow})/N$. A few simulations have been done also for $r_s = 40$, $\zeta = 1$. The electrons are placed in a square box with periodic boundary conditions. Long-ranged interactions are dealt with by a model potential [Eq. 68 of Ref. [16]] which has been shown to give smaller finite-size corrections than Ewald sums for the electron gas. The bias introduced by the finite population M of walkers and the finite time step τ was evaluated for selected systems and interpolated for all the others, according to standard procedures. To estimate the difference Δ between the energy $\epsilon_N(r_s, \zeta)$ of the finite system and its thermodynamic limit $\epsilon(r_s, \zeta)$, defined as $N \to \infty$ at fixed density, we adopted a less usual strategy. Rather than a separate size extrapolation for each density based on variational energies [4,5,14], we performed a global fit directly based on FN-DMC energies, which exploits two physically motivated ingredients: (i) the Fermi-liquid–like size correction [17]

$$\Delta(r_s,\zeta,N) = \epsilon_N(r_s,\zeta) - \epsilon(r_s,\zeta) = \delta(1+\lambda\zeta^2)[t_N(r_s,\zeta) - t_s(r_s,\zeta)] - (\eta+\gamma\zeta^2)/N \quad (1)$$

[t_N is the energy per particle of N noninteracting electrons confined in a 2D box of side $L=(N/n)^{1/2}$ with periodic boundary conditions, $t_s=(1+\zeta^2)/2r_s^2$ is equal to $\lim_{N\to\infty} t_N$ with n kept fixed, and $\delta,\lambda,\eta,\gamma$ are r_s-dependent parameters] and (ii) an analytic expression for $\epsilon(r_s,\zeta)$, detailed below, which involves 12 more free parameters. On these grounds, all the FN-DMC energies $\epsilon_N(r_s,\zeta)$ calculated here for $r_s=1$ to 10, plus those of Ref. [7] for $r_s=20$ and 30, plus the energy (independently extrapolated to the thermodynamic limit) for $r_s=40$, $\zeta=1$—a total of 122 data—formed the input for a best fit of the 36 free parameters, 24 of which disappear from the final analytic expression since they concern only the size extrapolation. This fit yields a reduced χ^2 of 3.8. More details will be reported elsewhere.

The fixed-node approximation is variational in character [3], and its accuracy depends on the nodal structure of Ψ. We choose a Slater-Jastrow trial function $\Psi(R)=J(R)D^{\uparrow}(R)D^{\downarrow}(R)$, where $R=\{\mathbf{r}_1,\ldots,\mathbf{r}_N\}$ represents the electronic coordinates, $J(R)=\exp[\sum_{i,j}u_{s_i,s_j}(r_{ij})]$ is a symmetric Jastrow factor with different pseudopotentials u_{s_i,s_j} for like- and unlike-spin pairs [18], and $D^{\uparrow(\downarrow)}$ is a Slater determinant for spin-up(down) electrons. The standard choice with homogeneous systems is to use plane waves (PW) as single-particle orbitals: $D^{\uparrow(\downarrow)}_{\mathrm{PW}}=\det[\exp(i\mathbf{k}_i\cdot\mathbf{r}_j)]$ [15]. However, within the fixed-node approximation, better results are obtained with backflow (BF) correlations in the wave function [14], $D^{\uparrow(\downarrow)}_{\mathrm{BF}}=\det[\exp(i\mathbf{k}_i\cdot\mathbf{x}_j)]$, with $\mathbf{x}_i=\mathbf{r}_i+\sum_{j\neq i}^{N}\eta_{\mathrm{BF}}(r_{ij})(\mathbf{r}_i-\mathbf{r}_j)$. Since BF simulations are considerably more demanding than those with PW determinants, we calculated BF energies only for $\zeta=0, N=58$ and $\zeta=1, N=57$ for each density, including correlation functions $\eta_{\mathrm{BF}}(r)$ as described in Ref. [14], optimized with variational Monte Carlo simulations [3] in each case. The expected error with BF nodes is much smaller than the difference between the PW and BF energies. For $r_s=1$, an exact calculation [19] shows agreement with the BF result within the statistical error. The BF results are compared with PW energies in Table I. For other values of N and ζ, the effect of backflow is estimated as a quadratic interpolation in ζ and appended to PW energies, under the further assumption that the size dependence is the same for BF and PW: the ~120 FN-DMC data used in the fit of Eq. (1) are the calculated PW energies, corrected for the time step and population bias, and shifted by the estimated backflow effect—the infinite-size extrapolation being given as a result of the fit.

As expected [7], BF correlations lower the energy more in the paramagnetic than in the polarized phase. At large r_s, this relative gain of the paramagnetic phase is a significant fraction of the difference in energy between the two phases.

Analytic representation for $\epsilon_c(r_s,\zeta)$.—We parametrize the energy $\epsilon(r_s,\zeta)$ as follows. We first noticed that the spin-polarization dependence of the exchange-correlation energy, $\epsilon_{xc}=\epsilon-t_s$, as given by the DMC data, is very well described by the simple form $c_0+c_1\zeta^2+c_2\zeta^4$ for $r_s\gtrsim 5$. On the other hand, the known high-density limit [20,21],

$$\epsilon_{xc}(r_s,\zeta)=\epsilon_x(r_s,\zeta)+a_0(\zeta)+b_0(\zeta)r_s\ln r_s+O(r_s), \quad (2)$$

contains non-negligible contributions from higher powers of ζ: the dominating exchange term ϵ_x is equal to $-2\sqrt{2}[(1+\zeta)^{3/2}+(1-\zeta)^{3/2}]/3\pi r_s$. Since we want to interpolate the energy between high and low density, we choose a functional form for the correlation energy $\epsilon_c=\epsilon_{xc}-\epsilon_x$ which quenches the contributions from ϵ_x beyond fourth order in ζ as r_s increases,

$$\epsilon_c(r_s\zeta)=(e^{-\beta r_s}-1)\epsilon_x^{(6)}(r_s,\zeta)+\alpha_0(r_s)+\alpha_1(r_s)\zeta^2+\alpha_2(r_s)\zeta^4, \quad (3)$$

where $\epsilon_x^{(6)}(r_s,\zeta)=\epsilon_x(r_s,\zeta)-(1+\frac{3}{8}\zeta^2+\frac{3}{128}\zeta^4)\times\epsilon_x(r_s,0)$ is the Taylor expansion of ϵ_x beyond fourth order in ζ. Since the first term on the right-hand side of Eq. (3) contains powers 6 and higher of ζ, it is immediate to identify the function $\alpha_0(r_s)$ as the correlation energy at zero polarization, $\alpha_0(r_s)=\epsilon_c(r_s,0)$. Furthermore, $\alpha_1(r_s)=2[\partial^2\epsilon_c(r_s,\zeta)/\partial\zeta^2]_{\zeta=0}$ (spin stiffness), and

TABLE I. FN-DMC energies with plane wave or backflow nodes. Data pertain to simulations with $N=58$ for $\zeta=0$ and $N=57$ for $\zeta=1$, $M=200$ and $\tau=0.002$, 0.01, 0.1, 0.3, 1.0, 2.0 in order of increasing r_s.

	Plane waves		Backflow	
r_s	$\zeta=0$	$\zeta=1$	$\zeta=0$	$\zeta=1$
1	−0.2013(1)	0.131 47(2)	−0.203 72(4)	0.131 09(4)
2	−0.255 802(4)	−0.193 349(1)	−0.257 21(3)	−0.193 59(2)
5	−0.149 134(9)	−0.143 520(5)	−0.149 518(9)	−0.143 610(7)
10	−0.085 270 6(4)	−0.084 555(2)	−0.085 427(6)	−0.084 584(2)
20	−0.046 241(1)	−0.046 238 5(6)	−0.046 283(1)	−0.046 248 8(8)
30	−0.031 923(1)	−0.031 929 8(6)	−0.031 941(2)	−0.031 938(1)

$\alpha_2(r_s) = 24[\partial^4 \epsilon_c(r_s,\zeta)/\partial\zeta^4]_{\zeta=0}$. Our choice for the functions $\alpha_i(r_s)$ is a generalization of the Perdew-Wang [22] form to the 2D case,

$$\alpha_i(r_s) = A_i + (B_i r_s + C_i r_s^2 + D_i r_s^3) \times \ln\left(1 + \frac{1}{E_i r_s + F_i r_s^{3/2} + G_i r_s^2 + H_i r_s^3}\right), \quad (4)$$

which features both the subleading contributions of the expansion (2) and terms in r_s^{-1} and $r_s^{-3/2}$ for $r_s \to \infty$ [23]. With suitable constraints, which leave only 12 independent parameters in Eqs. (3) and (4), our correlation energy satisfies exactly several known high-density and low-density limits: (i) the exact values [20,21] of $a_0(\zeta)$ and $b_0(\zeta)$ of Eq. (2) at $\zeta = 0$ and $\zeta = 1$, (ii) the vanishing of the correlation energy in the $r_s \to \infty$ limit, which implies that $D_i = -A_i H_i$, and (iii) the requirement that $\epsilon(r_s,\zeta)$ be independent of ζ for $r_s \to \infty$, recovering the low-density behavior $\epsilon \to -m/r_s + n/r_s^{3/2} + O(r_s^{-2})$ [23] with positive m and n independent of ζ.

The optimal values of the parameters are listed in Table II. In the high-density limit, we can compare the ζ dependence of our correlation energy with the exact one [20], finding very good agreement, as shown in the left panel of Fig. 1, where the widely used exchange-like interpolation [8] is also reported. In the right panel, we instead see the ζ dependence of the total energy at $r_s = 25.56$ where, according to our results, the transition to the fully polarized gas occurs. At such low densities, the exchange-like interpolation scheme (here performed using our energy values at $\zeta = 0$ and $\zeta = 1$) significantly deviates from the QMC result. Both predict a sudden transition from the $\zeta = 0$ to the $\zeta = 1$ fluid, but the energy barrier between the two phases given by QMC is more than an order of magnitude smaller, which reflects in a very large value of the spin susceptibility.

Spin susceptibility.—In our parametrization, the spin susceptibility χ of the ideal 2DEG is simply

$$\frac{\chi}{\chi_0} = \left[1 - \frac{\sqrt{2}}{\pi} r_s + 2 r_s^2 \alpha_1(r_s)\right]^{-1}, \quad (5)$$

TABLE II. Optimal fit parameters for the correlation energy, as parametrized in Eqs. (3) and (4). Values labeled with $*$ are obtained from exact conditions. The parameter $D_i = -A_i H_i$ is not listed (see text); the parameter β is equal to 1.3386.

	$i = 0$	$i = 1$	$i = 2$
A_i	-0.1925^*	$0.117\,331^*$	$0.023\,418\,8^*$
B_i	$0.086\,313\,6^*$	-3.394×10^{-2}	$-0.037\,093^*$
C_i	0.057 234	$-7.667\,65 \times 10^{-3*}$	$0.016\,361\,8^*$
E_i	1.0022	0.4133	1.424 301
F_i	$-0.020\,69$	0^*	0^*
G_i	0.340	$6.684\,67 \times 10^{-2}$	0^*
H_i	1.747×10^{-2}	7.799×10^{-4}	1.163 099

where α_1 is given by Eq. (4) and Table II. As mentioned, it turns out that χ is a very delicate quantity, so that different theoretical predictions significantly depart from each other at r_s as low as 3 or 4 [13].

In Fig. 2, we compare our result with other estimates of χ. The result of the Yarlagadda and Giuliani (YG) calculation [13] blows up already at $r_s \sim 4$. The tendency to predict a polarization transition at too high densities is shared by several approximate theories [13]. The exchange-like interpolation [8] is significantly lower than the QMC estimate, as expected from Fig. 1. Out of two recipes given in Ref. [4], based on a quadratic interpolation of the ζ dependence of the total energy (QI$\epsilon_{\rm tot}$) and of the correlation energy (QIϵ_c), respectively, the former (which yields by definition a divergent χ at the polarization density) is quite accurate for $r_s \lesssim 10$, whereas the latter greatly underestimates the spin-susceptibility at all but the smallest r_s (here the quadratic interpolation has been performed using our energy values at $\zeta = 0$ and $\zeta = 1$).

Our spin susceptibility is related to the second derivative of the model correlation energy, which incorporates an optimal interpolation of the QMC results and is constrained by known limiting behaviors at very low and very high densities. For this reason it represents a considerable progress over existing theories, providing a sound reference for further studies. Nevertheless, the precise value of χ at very large r_s (say, above 20) has to be taken with some caution. When the ζ dependence of $\epsilon(r_s,\zeta)$ is extremely weak (see the lower curve in the right panel of Fig. 1) the calculation of its derivatives is beyond the accuracy of the present calculation, due to the fixed-node bias, the assumption of quadratic contributions from BF correlation, possible uncertainties from the size extrapolation, statistical noise, and the chosen functional form of ϵ_c, Eq. (3). The very nature of the polarization transition, weakly first

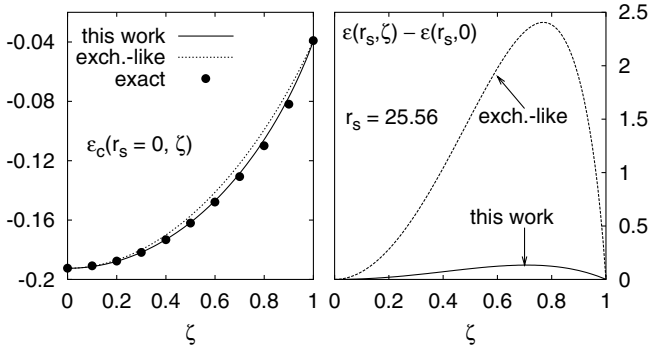

FIG. 1. Left panel: ζ dependence of the correlation energy in the high-density limit. Our result is compared with the exact values from Ref. [20] and with the exchange-like interpolation of Ref. [8]. Right panel: ζ dependence of the total energy at the polarization transition density, $r_s = 25.56$. The value at $\zeta = 0$ has been subtracted, and the result multiplied by 10^5. Our result is compared with the exchange-like interpolation.

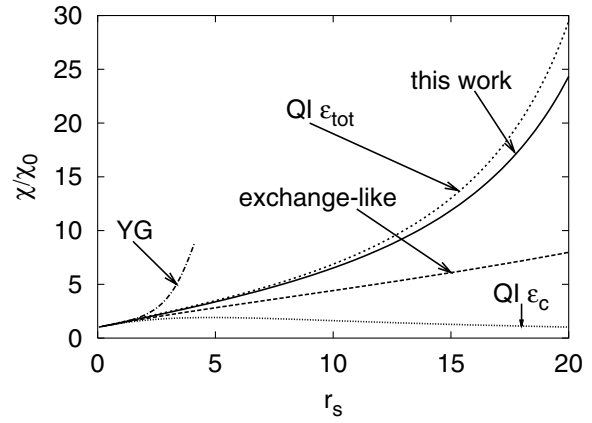

FIG. 2. Spin susceptibility for the 2DEG as a function of r_s. The present result is compared with the exchange-like approximation [8], with two quadratic interpolations [4] based on the total energy (QI$\epsilon_{\rm tot}$) and on the correlation energy (QIϵ_c), and with the YG [13] calculation.

order according to Fig. 1, is clearly based on the above approximations and assumptions.

Phase diagram.—The above results allow us to draw the zero-temperature phase diagram shown in Fig. 3, relative to the Wigner crystal, the paramagnetic liquid (PL), and the ferromagnetic liquid (FL). Intermediate-polarization phases never represent the stable phase in 2D (Ref. [7] and Fig. 1). For the fluid phases, the energy $\epsilon = t_s + \epsilon_{xc}$ is given by Eq. (3) with the parameters of Table II. The energy of the crystal is taken, instead, from Ref. [5], since neither backflow nor spin polarization play a significant role in the solid phase [24].

Similar FN-DMC studies, using plane-wave nodes, have been previously performed [4,5]. According to Ref. [4], crystallization occurs directly from the PL, although, at freezing, the energies of all three phases are very close to each other. Subsequent PW-based simulations [5,14] revised slightly upwards the energy of the PL, but this was enough to alter the previous result and to predict a small stability window for the FL [5]. Our backflow calculations lower back the energy of the PL relative to the FL, with the effect of shrinking, but apparently not eliminating, the density range where the FL phase is stable: the ideal 2DEG undergoes a polarization transition at $r_s \sim 26$, and the polarized liquid crystallizes at $r_s \sim 35$.

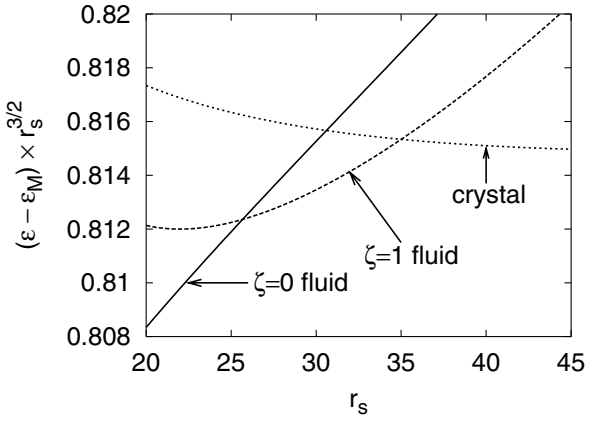

FIG. 3. r_s dependence of the ground-state energy ϵ of the 2DEG for the paramagnetic ($\zeta = 0$) and ferromagnetic ($\zeta = 1$) fluid phases, and for the Wigner crystal as given in Ref. [5]. $\epsilon_M = -1.1061/r_s$ is the Madelung energy.

We acknowledge support from MURST through COFIN99.

[1] T. Ando, A. B. Fowler, and F. Stern, Rev. Mod. Phys. **54**, 437 (1982).
[2] See, e.g., E. Abrahams, S. V. Kravchenko, and M. P. Sarachik, Rev. Mod. Phys. **73**, 251 (2001).
[3] M. Foulkes *et al.,* Rev. Mod. Phys. **73**, 33 (2001).
[4] B. Tanatar and D. M. Ceperley, Phys. Rev. B **39**, 5005 (1989).
[5] F. Rapisarda and G. Senatore, Aust. J. Phys. **49**, 161 (1996).
[6] J. Yoon *et al.,* Phys. Rev. Lett. **82**, 1744 (1999).
[7] D. Varsano, S. Moroni, and G. Senatore, Europhys. Lett. **53**, 348 (2001); D. Varsano, Ph.D. thesis, Università di Roma "La Sapienza," 2000 (unpublished).
[8] See, e.g., M. Koskinen, M. Manninen, and S. M. Reimann, Phys. Rev. Lett. **79**, 1389 (1997); S. M. Reimann *et al.,* Phys. Rev. Lett. **83**, 3270 (1999).
[9] See, e.g., B. Partoens and F. M. Peeters, Phys. Rev. Lett. **84**, 4433 (2000); K. Hirose and N. S. Wingreen, Phys. Rev. B **59**, 4604 (1999).
[10] Y.-H. Kim *et al.,* Phys. Rev. B **61**, 5202 (2000); L. Pollack and J. P. Perdew, J. Phys. Condens. Matter **12**, 1239 (2000); P. Garcia-González, Phys. Rev. B **62**, 2321 (2000).
[11] M. Ferconi and G. Vignale, Phys. Rev. B **50**, 14 722 (1994); O. Heinonen, J. M. Kinaret, and M. D. Johnson, Phys. Rev. B **59**, 8073 (1999).
[12] S. A. Vitkalov *et al.,* Phys. Rev. Lett. **87**, 86401 (2001).
[13] S. Yarlagadda and G. F. Giuliani, Phys. Rev. B **40**, 5432 (1989); see also B. Davoudi and M. P. Tosi, cond-mat/0107519, and references therein.
[14] Y. Kwon, D. M. Ceperley, and R. M. Martin, Phys. Rev. B **48**, 12 037 (1993).
[15] The chosen values of N, ranging from 21 to 114, correspond to closed shells of vectors $\mathbf{k}_i$ of the reciprocal lattice of the simulation box.
[16] L. M. Fraser *et al.,* Phys. Rev. B **53**, 1814 (1996).
[17] D. M. Ceperley, Phys. Rev. B **18**, 3126 (1978).
[18] G. Ortiz and P. Ballone, Phys. Rev. B **50**, 1391 (1994); **56**, 9970 (1997).
[19] Y. Kwon, D. M. Ceperley, and R. M. Martin, Phys. Rev. B **53**, 7376 (1996).
[20] M. Seidl and J. P. Perdew (unpublished).
[21] A. K. Rajagopal and J. C. Kimball, Phys. Rev. B **15**, 2819 (1977); A. Isihara and L. Ioriatti *ibid.* **22**, 214 (1980).
[22] J. P. Perdew and Y. Wang, Phys. Rev. B **45**, 13 244 (1992).
[23] L. Bonsall and A. A. Maradudin, Phys. Rev. B **15**, 1959 (1977).
[24] We performed simulations for the solid phase at $r_s = 30$ and 40. Our results for $N = 56$ particles agree with the ones of Ref. [5], while showing small discrepancies with Ref. [4].